OPTIMIZATION OF A HYBRID HEATING SYSTEM COMBINING AN AIR SOURCE HEAT PUMP AND WATER STORAGE IN NORTHWEST CHINA

by

Xiaolong WANG *

CHN Energy Shendong Coal Group Co., Ltd., Inner Mongolia, China

Original scientific paper
https://doi.org/10.2298/TSCI2503899W

In order to address the issue of inadequate heating in the northwest region of China, a hybrid heating system combining an air source heat pump and water storage is proposed. The proposed operation strategy and heating regulation mode are implemented in a water storage heating system and a hybrid heating system combining air source heat pump and water storage constructed using TRNSYS software. The optimization design is carried out with the annual cost value as the objective function. As a case study, the results demonstrate that the initial investment of the water storage thermoelectric boiler heating system increases with the increase of the heat storage ratio, while the annual operating cost decreases with the increase of the heat storage ratio. When the increased equivalent annual cost during the heating season exactly offsets the reduced annual operating cost, the optimal heat storage ratio is achieved. Furthermore, the optimal system is discussed. From the standpoint of comprehensive economic and energy conservation, the hybrid heating system exhibits notable advantages.

Key words: *air source heat pump, heat storage system, TRNSYS model, optimal design*

Introduction

The majority of heating systems in northern China are powered by coal, resulting in significant emissions of smoke and severe environmental contamination [1]. The *dual carbon targets* are imminent, and their achievement depends on the energy consumption of the construction industry [2]. According to statistics, the construction industry accounted for 50.9% of the China's carbon emissions in 2020 [3], and refrigeration and heating are the main sources of building energy consumption [4]. Concurrently, as living standards improve, the expectations of the living environment are elevated, leading to a rapid increase in energy consumption [5]. This not only creates a peak-valley difference in the power grid [6] but also presents significant challenges to the realization of the dual carbon goal. In response to these challenges, air source heat pumps (ASHP) are increasingly utilized as an economical, energy-saving, and pollution-free heating method [7]. The ASHP utilize ambient air to provide heat [8], and can be broadly classified into two categories: air-water heat pumps and air-air heat pumps. In terms of economics, air-water heat pumps are more cost-effective than air-air heat pumps, which are more suitable for modern heating systems [9, 10].

* Author's e-mail: kelseydong@tzc.edu.cn

Although ASHP exhibit favorable economic efficiency, they are susceptible to frosting when operating in low ambient temperature and high humidity environments. Furthermore, an increase in compressor compression ratio results in a decline in system performance, rendering the heat pump unable to fulfill the heating needs of users. A considerable number of scholars have conducted research on ASHP heating. By developing technical and economic models for ASHP heating, Zhang *et al.* [11] demonstrated the viability of low temperature ASHP in cold and severe cold regions. Ma *et al.* [12] investigated the ASHP system with local cooling of the scroll compressor, which addressed the heating issue in North China to a certain extent. Dong *et al.* [13] and Yang *et al.* [14] enhanced the heating efficacy of ASHP through the RCD thermal storage method. In conclusion, the majority of research has focused on the ASHP unit itself, with relatively little research conducted on its operating system. In light of the suboptimal heating performance of ASHP at low ambient temperatures, this paper proposes an ASHP water storage hybrid heating system by incorporating a stable and straightforward storage water boiler into the heating system. The hourly heat load and operational strategy of the building are taken into account when TRNSYS software is used to establish a storage water boiler heating system and an ASHP water storage hybrid heating system. The annual cost is taken as the objective function in order to compare and analyze the economic efficiency of the two heating systems, as well as to analyze the environmental benefits.

System principle and operation strategy

The ASHP is characterized by stable operation and high economic efficiency, rendering it an optimal choice as the primary heat source at the outset and conclusion of the heating cycle. However, during the middle of the heating period, the heating capacity of ASHP units will significantly decline. Therefore, this paper proposes the use of water-storage thermoelectric boilers as an auxiliary heating source. The schematic representation of the heating system is depicted in fig. 1.

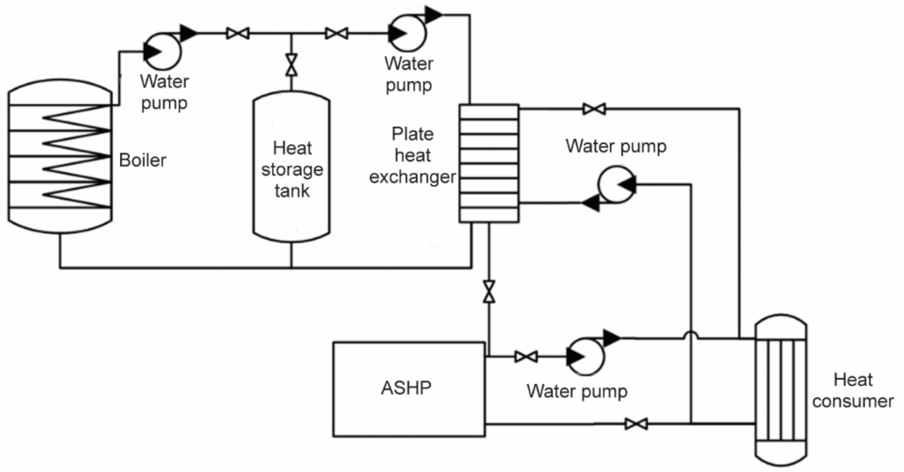

Figure 1. Principle of hybrid system combined ASHP and water-storage boiler

The operational strategy of the hybrid heating system, which combines an ASHP with a water storage boiler, is as follows: At the beginning and end of the heating season, the thermoelectric boilers are deactivated, and the ASHP are directly responsible for providing the heat users with hot water. In the middle of the heating season, the ASHP first heat the water to a specified temperature, then mix it with the high temperature effluent from the thermoelectric boiler or thermal storage tank, and finally supply it to the heating users. Among these, the thermal storage tank is the preferred means of providing auxiliary heating. If the set-point value of the water supply temperature has not yet been reached, the thermoelectric boilers will be activated for heating purposes until the desired temperature for the water has been achieved.

Mathematical model

The mathematical model of the main equipment of the system

Mathematical model of thermoelectric boiler

The heat produced by a thermoelectric boiler can be expressed:

$$Q_\mathrm{B} = Q_\mathrm{P}\eta_\mathrm{B} \tag{1}$$

where Q_B [kW] is the heat produced by the thermoelectric boiler, Q_P [kW] – the input power of thermoelectric boiler, and η_B – the overall efficiency of the thermoelectric boiler.

The outlet water temperature of the thermoelectric boiler can be expressed:

$$t_\mathrm{out,B} = t_\mathrm{in,B} + \frac{Q_\mathrm{B}}{\dot{m}_\mathrm{B} c_p} \tag{2}$$

where $t_\mathrm{out,B}$ [°C] is the outlet water temperature of the thermoelectric boiler, $t_\mathrm{in,B}$ [°C] – the inlet water temperature of the thermoelectric boiler, $\dot{m}_\mathrm{B}$ [kgs^{-1}] – the mass-flow rate of circulating water of the thermoelectric boiler, and c_p [kJkg^{-1}°C^{-1}] – the specific heat capacity of water.

Mathematical model of heat storage tank

The temperature stratification of the heat storage tank can be modelled using a multi-node method. The heat storage water tank is vertically divided into multiple layers, with each layer corresponding to a temperature node.

The energy balance equation for node i can be expressed:

$$\dot{m}_\mathrm{s}\frac{\mathrm{d}T_{i,\mathrm{H}}}{\mathrm{d}t} = \dot{m}_\mathrm{s}(T_\mathrm{s} - T_{i,\mathrm{H}}) - \dot{m}_\mathrm{L}(T_{i,\mathrm{H}} - T_\mathrm{L,r}) - \frac{UA}{c_p}(T_{i,\mathrm{H}} - T_\mathrm{a}) + Q_{i,\mathrm{m}} \tag{3}$$

$$Q_{i,\mathrm{m}} = \dot{m}_{i,\mathrm{m}}(T_{i-1,\mathrm{H}} - T_{i,\mathrm{H}}) \tag{4}$$

where $\dot{m}_\mathrm{S}$ [kgs^{-1}] is the average mass-flow rate of supply water on the heat source side, $T_{i,\mathrm{H}}$ [°C] – the water temperature of node i of the heat storage tank, T_s [°C] – the temperature of supply water, $\dot{m}_\mathrm{L}$ [kgs^{-1}] – the average mass-flow rate of the return water on the load side, $T_\mathrm{L,r}$ [°C] – the return water temperature on the load side, U – the heat loss coefficient of the heat storage tank, A [m^2] – the surface area of the heat storage tank in contact with the environment, c_p [kJkg^{-1}°C^{-1}] – the specific heat capacity of water, T_a [°C] – the ambient temperature, $Q_{i,\mathrm{m}}$ [kJs^{-1}] – the net exchange heat caused by mixing between nodes, and $\dot{m}_{i,\mathrm{m}}$ [kgs^{-1}] – the net flow from node i-1 to node i.

Mathematical model of ASHP

The outlet temperature of the ASHP can be expressed:

$$T_{\mathrm{w,out}} = T_{\mathrm{w,in}} + \frac{\dot{Q}_{\mathrm{h,air}}}{\dot{m}_{\mathrm{w}} Cp_{\mathrm{w}}} \tag{5}$$

where $T_{\mathrm{w,out}}$ [°C] is the outlet water temperature of the ASHP, $T_{\mathrm{w,in}}$ [°C] – the inlet water temperature of the ASHP, $\dot{Q}_{\mathrm{h,air}}$ [kJs^{-1}] – the total heat produced by the ASHP, $\dot{m}_{\mathrm{w}}$ [kgs^{-1}] – the mass-flow rate of circulating water, and Cp_{w} [kJkg^{-1}°C^{-1}] – the specific heat capacity of heating fluid.

Evaporator side refrigerant heat absorption is computed:

$$\dot{Q}_{\mathrm{e}} = \dot{Q}_{\mathrm{h,air}} - \dot{P}_{\mathrm{com}} \tag{6}$$

where $\dot{Q}_{\mathrm{e}}$ [kJs^{-1}] is the ASHP refrigerant heat absorption and $\dot{P}_{\mathrm{com}}$ [kJs^{-1}] – the rated power of the compressor of the ASHP unit.

Assuming that the humidity ratio of outlet air remains constant, the enthalpy value of outlet air on the evaporator side is given by:

$$h_{\mathrm{air,out}} = h_{\mathrm{air,in}} - \frac{\dot{Q}_{\mathrm{e}}}{\dot{m}_{\mathrm{air}}} \tag{7}$$

where $h_{\mathrm{air,out}}$ [kJkg^{-1}] is the outlet air enthalpy value of the ASHP evaporator, $h_{\mathrm{air,in}}$ [kJkg^{-1}] – the inlet air enthalpy value of the ASHP evaporator, and $\dot{m}_{\mathrm{air}}$ [kJs^{-1}] – the outdoor air mass-flow rate.

Enthalpy value of outdoor air after heat absorption is computed:

$$h_{\mathrm{f,out}} = h_{\mathrm{air,out}} - \frac{\dot{P}_{\mathrm{f}}}{\dot{m}_{\mathrm{air}}} \tag{8}$$

where $h_{\mathrm{f,out}}$ [kJkg^{-1}] is the enthalpy of air at the outlet of the heat pump fan and $\dot{P}_{\mathrm{f}}$ [kJkg^{-1}] – the rated power of the heat pump fan.

Total outdoor air energy consumption is given by:

$$\dot{Q}_{\mathrm{total,air}} = \dot{m}_{\mathrm{air}} (h_{\mathrm{f,out}} - h_{\mathrm{air,in}}) \tag{9}$$

where $\dot{Q}_{\mathrm{total,air}}$ [kJs^{-1}] is the total outdoor air energy consumption.

The heating performance coefficient of ASHP is calculated by:

$$COP_{\mathrm{h}} = \frac{\dot{Q}_{\mathrm{h,air}}}{\dot{P}_{\mathrm{com}} + \dot{P}_{\mathrm{f}}} \tag{10}$$

where COP_{h} is the heating performance coefficient of ASHP.

Heat source allocation ratio

The optimization of the heat source in a heating system is intended to address the discrepancy between the capacity of the equipment and the actual system, which can result in significant investment and economic implications. A reasonable determination of the heat source configuration scheme can reduce the capacity of the heat storage tank, thermoelectric boiler and ASHP, thereby reducing the project cost to the greatest extent possible while ensuring that the requirements of users are met. In order to facilitate the analysis, the concepts of heat storage ratio and ASHP configuration ratio are introduced in this study.

The heat storage ratio of the water storage heating system is defined:

$$X = \frac{\dot{Q}_{\mathrm{st}}}{L_{\mathrm{d}}} \tag{11}$$

where X is the heat storage ratio of the water storage heating system, $\dot{Q}_{\mathrm{st}}$ [kWh^{-1}] – the amount of heat provided by the heat storage tank, and L_{d} [kWh^{-1}] – the heat load of the building in the design day.

The heat storage ratio of the hybrid heating system is defined:

$$X_k = \frac{\dot{Q}_{\mathrm{st}}}{L_{\mathrm{d}} - Q_{\mathrm{hp}}} \tag{12}$$

where X_k is the heat storage ratio of the hybrid heating system and Q_{hp} [kWh^{-1}] – the amount of heat provided by the ASHP.

The ASHP configuration ratio K is defined:

$$K = \frac{P_k}{P_{k,\,\max}} \tag{11}$$

where K is the ASHP configuration ratio, P_k [kW] – the capacity of ASHP in the hybrid heating system, and $P_{k,\max}$ [kW] – the maximum hourly heat load of the hybrid heating system in the design day.

Objective function

From the perspective of engineering project analysis, life cycle cost (LCC) includes decision-making costs, construction costs, operation costs, and maintenance costs. This method is comprehensive and forward-looking, which not only helps maximize the economic benefits of engineering projects, but also helps ensure the sustainability and standardization of engineering projects, facilitating intuitive display of their evaluation indicators. Therefore, this method is of great significance to engineering projects. In order to optimize the hybrid heating system, the influence of time-of-use electricity prices, heat storage rates, and heat source configuration rates on annual cost values was studied from the perspective of LCC. The mathematical expression of the entire life cycle cost can be expressed:

$$LCC_{\min} = \min(C_t + C_n) \tag{14}$$

where LCC [CNY] is the annual cost value of the heating design scheme, C_t [CNY] – the initial investment in the heating design scheme, and C_n [CNY] – the annual operating cost of the heating design scheme in the normal service life.

In order to analyze and compare the initial investment and operating costs, the initial investment of the heating system is converted into an equivalent annuity according to the service life of the equipment. This can be expressed:

$$C_t = C_c \frac{a(1+a)^f}{(1+a)^f - 1} \tag{15}$$

where C_c [CNY] is the initial investment cost in the heating system, a – the benchmark discount rate, and f [years] – the service life of the equipment.

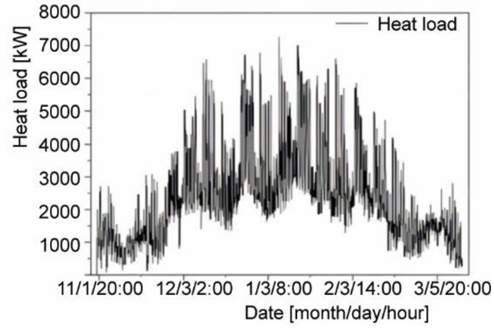

Figure 2. Hourly heat load

Case study

Architectural overview

The total heating area of the energy station is 120000 m², and 13 heat exchange stations are supplied from the heat source. The period of heating is from November 1 to March 15 of the following year. The TRNSYS software was employed to calculate the hourly heat load of the region which is illustrated in fig. 2. It can be observed that the maximum heating load occurred on January 7th of the following year. The cumulative maximum daily heat load is 115222.7 kW, while the annual cumulative heat load is 7537972.2 kWh.

Model building

In this study, the water supply and return temperature of the storage tank is 95/50 ℃, the water supply and return temperature of the primary side is 60/50 ℃, and the primary network employs phased mass regulation. The water supply and return temperature of the secondary side is 55/45 ℃, and the secondary network employs quality regulation. The indoor temperature of the building heating is set at 18 ℃, and the heating terminals are radiators.

The regulation of the heating system is illustrated in fig. 3.

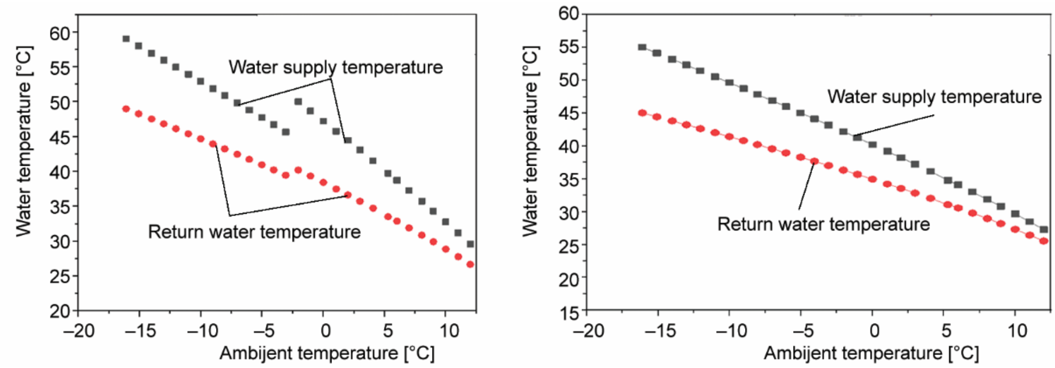

Figure 3. Heating supply regulation

Study on optimization of heating system

Analysis of impact of variations of heat storage ratio in water storage heating system

According to the previous model, the annual cost value of heat storage ratio is calculated at 10% interval, as shown in fig. 4.

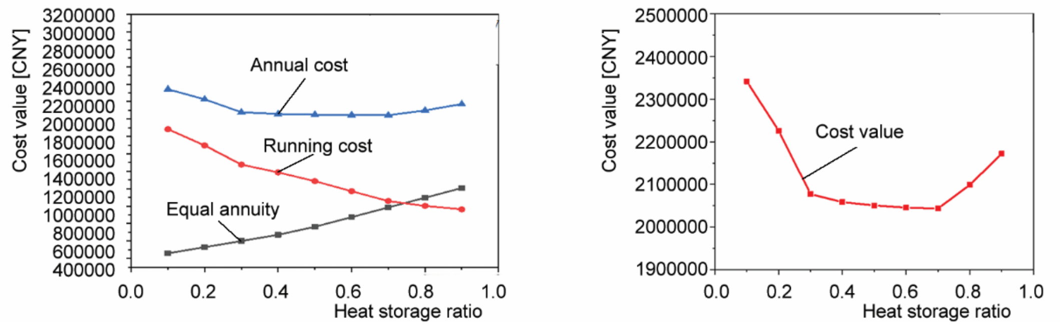

Figure 4. Relationship between heat storage ratio and cost value

It is evident that the total cost reaches a minimum within the range of 60% to 80% of the heat storage ratio. In other words, there exists an optimal heat storage ratio. Then the initial investment, operating cost and total cost are calculated in 1% increments. The results are shown in fig. 5.

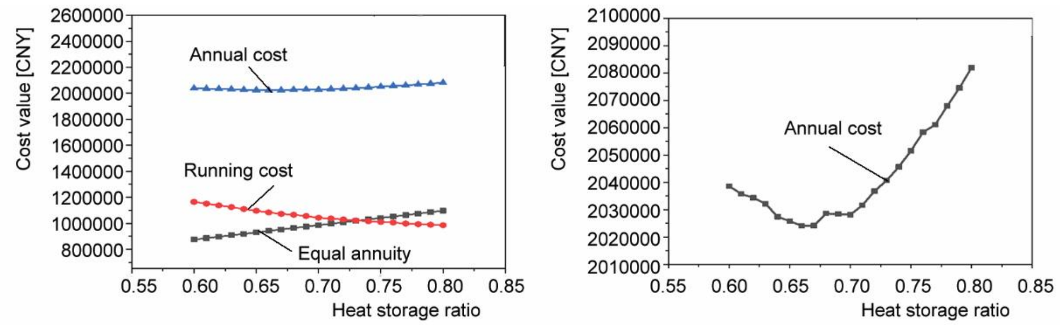

Figure 5. Relationship between heat storage ratio and cost value

Figures 4 and 5 demonstrate that the initial investment of the water storage heating system increases with the rise in the heat storage ratio. Furthermore, the rate of increase accelerates after a certain point. This is due to the increase in initial investment is only attributed to the increase in the capacity of the thermal storage tank. However, when the maximum power of the thermoelectric boiler during the valley power stage is greater than the maximum power of the thermoelectric boiler during the peak power stage, the increase in initial investment is caused by the increase in the capacity of the thermoelectric boiler and the thermal storage tank. In addition, the capacity of the thermoelectric boiler also begins to increase with the increase in thermal storage ratio, resulting in a faster increase rate.

As the heat storage ratio increases, the annual operating cost decreases at a gradually slowing rate. This occurs because the heat load during most daily peak hours in the heating season is less than the designed daily heat load. As the heat storage ratio increases, the heat stored during the off-peak hours largely substitutes for the heat load during the peak hours. When the heat storage ratio continues to increase, the heat load during the peak hours in the early and late stages of the heating season can be fully offset by the energy stored during the off-peak hours. Continued increases in heat storage will primarily supplement the heat load during the off-peak hours, thereby slowing the decrease in annual operating costs.

As the heat storage ratio increases, the annual cost initially decreases and then increases. When the initial investment is balanced with the decrease in annual operating costs, the optimal heat storage ratio is achieved. In this heating system, the optimal heat storage ratio is 67%, and the minimum cost is 2024100 CNY.

Analysis of impact of variations of heat storage ratio in hybrid heating system

Figure 6 illustrates the annual cost value for a hybrid heating system under different ASHP configuration ratios and different heat storage ratios. When $X_k = 0.1$, the optimal heat pump ratio K is 0.3. Conversely, when $X_k = 1$, the optimal heat pump ratio K is 0.4. As X_k increases, the annual cost of the heat source scheme with a smaller K value initially decreases and then increases. This indicates the existence of an optimal ASHP configuration ratio. Due to the priority given to using ASHP to meet building thermal load, the operating time of the thermal storage heating system has been reduced, resulting in an increase in the annual cost of the heat source scheme with a larger K value. In addition, the implementation of thermal storage devices lowers the operating cost of the hybrid heating system, this advantage fails to compensate for the initial investment and additional costs associated with the thermal storage tank.

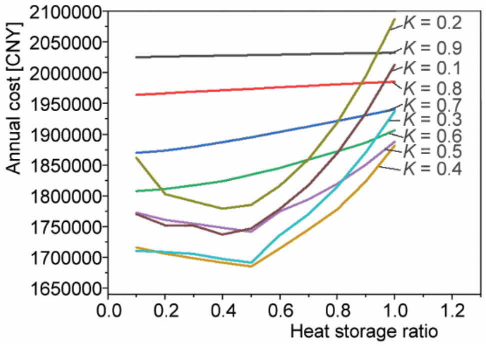

Figure 6. Relationship between allocation ratio of ASHP and annual cost value

As the ASHP configuration ratio increases, the load borne by ASHP gradually increases, while the load borne by the water storage heating system gradually decreases. Consequently, the operating cost of the hybrid heating system becomes less affected by the heat storage ratio. Given the significant initial investment required for ASHP, the annual cost is expected to increase with the increase in the heat storage ratio, particularly when the ASHP configuration ratio is relatively large. The results of the simulation indicate that the annual cost of the hybrid heating system is at its minimum when $X_k = 0.5$ and $K = 0.4$, amounting to 1.685 million CNY.

Discussion and conclusions

The hybrid heating system is systematically studied, the principal findings are as follows.

- For the heating system, TRNSYS software components were employed to optimize the overall system model. The system improves the economy of heat supply to a certain extent by regulating heat supply and using low energy to store heat.
- The heating system has an optimal heat storage ratio, which is generally reached when the increase in the initial investment equivalent annuity is balanced by the decrease in the annual operating cost. When the optimal ASHP configuration ratio is 0.4 and optimal heat storage ratio is 0.5, the annual cost of the hybrid heating system is the smallest, with a minimum of 1.685 million CNY.

Although the hybrid heating system can be optimized and its efficiency has been greatly improved, there is still much room to further improve the system by using nanofluids

[15, 16]. Metal nanoparticles in the heating fluid can greatly enhance the heat transfer across the interface [17, 18].

References

[1] Wang, H., *et al.*, Test Investigation of Operation Performance of Novel Split-Type Ground Source Heat Pump Systems for Clean Heating of Rural Households in North China, *Renewable Energy*, *163* (2021), Jan., pp. 188-197
[2] Liu, Z., *et al.*, Challenges and Opportunities for Carbon Neutrality in China, *Nature Reviews Earth and Environment*, *3* (2022), 2, pp. 141-155
[3] ***, CABEE, China's Building Energy Consumption and Carbon Emissions Research Report 2022, Chongqing. https://mp.weixin.qq.com/s/7Hr__rkhS70owqTbYI_XuA
[4] Gan, L., *et al.*, Regional Inequality in the Carbon Emission Intensity of Public Buildings in China, *Building and Environment*, *225* (2022), Nov., pp. 1-11
[5] Yao, X., *et al.*, Can Urbanization Process and Carbon Emission Abatement be Harmonious? New Evidence from China, *Environmental Impact Assessment Review*, *71* (2018), July, pp. 70-83
[6] Wang, X., *et al.*, Employing Cationic Kraft Lignin as an Electrolyte Additive to Enhance the Electrochemical Performance of Rechargeable Aqueous Zinc-Ion Battery, *Fuel*, *333* (2023), 126450
[7] Deng, M., *et al.*, Techno-Economic Performances of Clean Heating Solutions to Replace Raw Coal for Heating in Northern Rural China, *Energy and Buildings*, *240* (2011), 110881
[8] Brenn, J., *et al.*, Comparison of Natural Gas Driven Heat Pumps and Electrically Driven Heat Pumps with Conventional Systems for Building Heating Purposes, *Energy and Building*, *42* (2010), 6, pp. 904-908
[9] Zhao, N., You, F., Can Renewable Generation, Energy Storage and Energy Efficient Technologies Enable Carbon Neutral Energy Transition? *Applied Energy*, *279* (2020), 115889
[10] Wang, W., *et al.*, Performances of ASHP System for a Kind of Mal-Defrost Phenomenon Appearing in Moderate Climate Conditions, *Applied Energy*, *112* (2013), Dec., pp. 1138-1145
[11] Zhang, Q. L., *et al.*, Techno-Economic Analysis of Air Source Heat Pump Applied for Space Heating in Northern China, *Applied Energy*, *207* (2017), Dec., pp. 533-542
[12] Ma, G., *et al.*, Experimental Investigation of Air-Source Heat Pump for Cold Regions, *International Journal of Refrigeration*, *26* (2003), 3, pp. 12-18
[13] Dong, J. K., *et al.*, Defrosting Performances of a Multi-Split ASHP with Phase Change Thermal Storage, *International Journal of Refrigeration*, *55* (2015), July, pp. 49-59
[14] Yang, B., *et al.*, Heating and Energy Storage Characteristics of Multi-Split ASHP Based on Energy Storage Defrosting, *Applied Energy*, *238* (2019), Mar., pp. 303-310
[15] Pourfayaz, F., *et al.*, Numerically Investigating the Effect of Using Nanofluids on the Thermal Performance and Coefficient of Performance of a U-Tube Deep Borehole Ground Source Heat Pump, *Geoenergy Science and Engineering*, *238* (2024), 212890
[16] Narei, H., *et al.*, The Effect of Employing Nanofluid on Reducing the Bore Length of a Vertical Ground-Source Heat Pump, *Energy Conversion and Management*, *123* (2016), Sept., pp. 581-591
[17] He, J. H., *et al.*, Efficacy of a Modulated Viscosity-Dependent Temperature/Nanoparticles Concentration Parameter on a Non-linear Radiative Electromagneto-Nanofluid Flow Along an Elongated Stretching Sheet, *Journal of Applied and Computational Mechanics*, *9* (2023), 3, pp. 848-860
[18] He, J. H., Abd-Elazem, N. Y., The Carbon Nanotube-Embedded Boundary Layer Theory for Energy Harvesting, *Facta Universitatis, Series: Mechanical Engineering*, *20* (2022), 2, pp. 211-235

Paper submitted: April 15, 2024
Paper revised: July 7, 2024
Paper accepted: July 7, 2024